Achieving Full-View Coverage in Camera Sensor Networks

YI WANG and GUOHONG CAO, Pennsylvania State University

Camera sensors are different from traditional scalar sensors, as cameras at different positions can form very different views of the object. However, traditional coverage model does not consider this intrinsic property of camera sensors. To address this issue, a novel model called full-view coverage is proposed. It uses the angle between the object's facing direction and the camera's viewing direction to measure the quality of coverage. An object is full-view covered if there is always a camera to cover it no matter which direction it faces and the camera's viewing direction is sufficiently close to the object's facing direction. An efficient method is proposed for full-view coverage detection in any given camera sensor networks, and a sufficient condition on the sensor density needed for full-view coverage in a random uniform deployment is derived. In addition, the article shows a necessary and sufficient condition on the sensor density for full-view coverage in a triangular lattice-based deployment. Based on the full-view coverage model, the article further studies the barrier coverage problem. Existing weak and strong barrier coverage models are extended by considering direction issues in camera sensor networks. With these new models, weak/strong barrier coverage verification problems are introduced, and new detection methods are proposed and evaluated.

Categories and Subject Descriptors: C.2.2 [**Computer-Communication Networks**]: Network Protocols

General Terms: Design, Algorithms, Theory

Additional Key Words and Phrases: Camera sensor networks, full-view coverage, barrier coverage, coverage verification

ACM Reference Format:
Wang, Y. and Cao, G. 2013. Achieving full-view coverage in camera sensor networks. ACM Trans. Sensor Netw. 10, 1, Article 3 (November 2013), 31 pages.
DOI: http://dx.doi.org/10.1145/2529974

1. INTRODUCTION

Traditional sensor networks measure scalar phenomena in the physical world. Camera sensor networks can retrieve much richer information in the form of images or videos, and hence provide more detailed and interesting data of the environment. Such networks promise a wide range of applications in surveillance, traffic monitoring, habitat monitoring, healthcare, and even online gaming [Akyildiz et al. 2007; Rinner and Wolf 2008; Soro and Heinzelman 2009]. Because of the huge potential in many applications, camera sensor networks have received considerable attention in the past few years.

One fundamental research issue is how well the target field is monitored, which is referred to as the coverage problem in wireless sensor networks. Existing works on

This article is based in part on work presented in *Proceedings of the 30th IEEE International Conference on Computer Communications (INFOCOM'11)* [Wang and Cao 2011c], and part on work presented in *Proceedings of the 12th ACM International Symposium on Mobile Ad Hoc Networking and Computing (MobiHoc'11)* [Wang and Cao 2011a].
This work was supported in part by the National Science Foundation under grant CNS-0916171.
Authors' addresses: Y. Wang (corresponding author) and G. Cao, Department of Computer Science and Engineering, Pennsylvania State University, University Park; corresponding author's email: yuw124@psu.edu.

DOI: http://dx.doi.org/10.1145/2529974

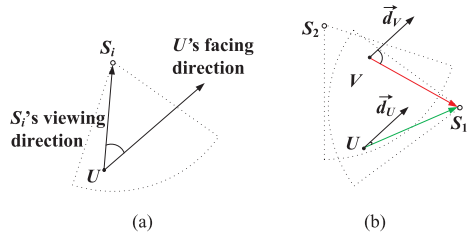

Fig. 1. (a) U is an object; dotted line defines the sensing range of camera sensor S_i and $\vec{US_i}$ is its viewing direction of the object; (b) although U and V's facing directions, $\vec{d_U}$ and $\vec{d_V}$, are the same, S_1's viewing direction is closer to U's facing direction.

this problem suggest a very simple model on characterizing the coverage: an object is considered to be covered if it is within the sensor's sensing range, which can be either a disk [Wang et al. 2003; Cardei and Wu 2006; Liu and Cao 2011] or a sector [Cai et al. 2009; Wang and Cao 2011b]. With this model, studies have been devoted to the problem of how to achieve k-coverage over a given area, where k is a predefined parameter indicating the desired number of sensors (coverage degree) covering each object.

However, camera sensors are different from traditional scalar sensors. Camera sensors may generate very different views of the same object if they are from different viewpoints. For example, a camera sensor placed in front of a person can obtain the face image, but it can only see his back if it is behind him. In fact, studies in computer vision show that the object is more likely to be recognized by the recognition system if the image is captured at or near the frontal viewpoint [Blanz et al. 2005], that is, when the object is facing straight to the camera. As the angle between the object's facing direction and the camera's viewing direction (denoted by the vector from the object to the camera, as shown in Figure 1(a)) increases, the detection rate drops dramatically [Sanderson et al. 2007; Phillips et al. 2007]. As a result, the viewing direction of the sensor has significant impact on the quality of coverage in camera sensor networks.

As none of the existing coverage models can be used to address the issues of viewing direction, we propose a novel model called *full-view coverage*. An object is said to be full-view covered if no matter which direction the object faces, there is always a sensor whose sensing range covers the object and the sensor's viewing direction is sufficiently close to the object's facing direction (rigorous definition will be given in Section 2). Informally, if an area is full-view covered, it is guaranteed that every aspect of an object at any position is under the view of the camera sensor network.

With this model, we study coverage problems arising in camera sensor networks. One important problem is that given a deployed camera sensor network, how to determine if the monitored field is full-view covered? Compared to the traditional model, there are two factors that increase the complexity of the problem in full-view coverage. First, the sensing range of a camera sensor is a sector rather than a unit disk. Second, and more importantly, the viewing direction of each camera sensor can vary from one position to another, and hence even if the objects are covered (in traditional sense) by the same set of camera sensors, they may receive different quality of coverage due to the variance in position. For example, in Figure 1(b), both objects U, V are covered by camera sensors S_1 and S_2, and they are facing the same direction. However, the viewing direction of S_1 is closer to U's facing direction than to V's, meaning that U receives better coverage (more likely to be recognized) than V. On top of that, there are infinite number of positions to be considered in the monitored field and the object can face any direction at any point, which further increases the difficulty.

Another important problem is how to derive an estimate of the sensor density needed in a real deployment for full-view coverage. In practice, sensors can be either deployed

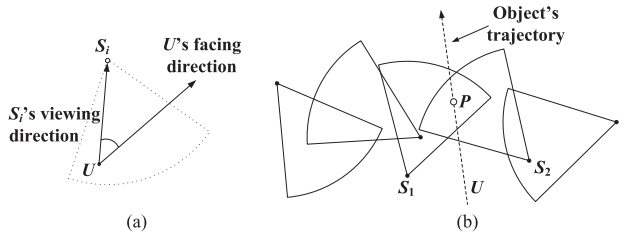

Fig. 2. (a) U is an object; dotted line is the sensing range of S_i and $\vec{US_i}$ is the viewing direction of S_i; (b) if U faces the direction along the trajectory (forward), S_1 and S_2 are not able to view its face, although U is within their coverage.

randomly, for example, being dropped from an aircraft to an inaccessible zone, or deployed deterministically, for example, being placed manually in a controlled environment. In both cases, a reliable estimation can serve as a guideline for the deployment in practice. Since most previous works mainly focus on disk sensing model, no result can be applied directly on full-view coverage, where combined effects of the distance, camera's orientation, and viewing direction make the geometric relationship between the objects and the sensors more complex, and hence make the problem much more challenging.

The problems discussed so far are on the coverage of a whole area. It is imaginable that full-view coverage of the whole area requires significant number of camera sensors to be deployed. Given the relatively high cost of the camera sensors, it is helpful to consider the barrier coverage model [Kumar et al. 2005]. Barrier coverage is an important concept proposed for various sensor network applications, for example, national border control, critical resource protection, security surveillance, and intruder detection. In a wireless sensor network, a barrier is formed by a set of sensors whose sensing ranges are connected and span (usually a strip area) across the monitored field. Every object traversing the field from one side to another will be detected by the sensors on the barrier. Compared with full coverage (covering the whole area), the number of sensors required for barrier coverage is much less. Hence barrier coverage is considered more scalable and attractive for many practical applications.

While previous studies on barrier coverage mainly focused on traditional scalar sensor networks, the barrier coverage in camera sensor networks is much different and more complicated. Simply combining the sensing range of a series of cameras across the monitored field does not provide effective barrier coverage. This is because an intruder may cross the barrier without being identified, that is, its *face* image could be missed (Figure 2). Therefore, the barrier coverage problem of camera sensor networks deserve careful study.

In this article, we study the barrier coverage problem of camera sensor networks based on the full-view coverage model. We consider two notations of barrier coverage defined in literature: the weak barrier coverage and the strong barrier coverage [Kumar et al. 2005]. In weak barrier coverage, the object is assumed to take a shortest path to cross the field, but in strong barrier coverage, the object is assumed to take any possible paths between the entrance and the exit. Weak barrier coverage demands fewer number of sensors, while strong barrier coverage provides better coverage.

In our study of camera sensor networks, these two notations of barrier coverage are extended by considering direction issues, and new barrier coverage models are proposed. Besides choosing the traversing path as in the existing models, the object may have some flexibility to choose where to face (or how it is observed). The stronger the model is, the more choices the object is allowed to have on where to face and how to cross the field (detailed definitions given later in Sections 6 and 7), and hence demanding more sensor resources to achieve the desired coverage.

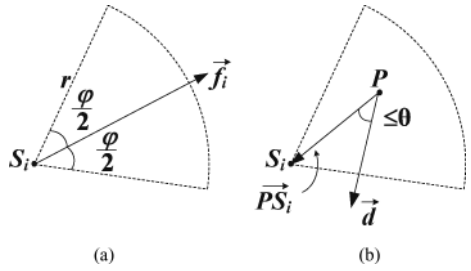

Fig. 3. The full-view coverage model.

With new weak and strong barrier coverage models, we need to address the barrier coverage verification problem. Given a deployed camera sensor network, we need to determine if the monitored field is under proper barrier coverage. This is straightforward in a traditional disk sensing model, since it is sufficient to just check if the sensing range of the sensors is connected and across the field. However, it can not be applied for camera barrier due to the direction issues just discussed. Hence new techniques for barrier coverage verification are needed.

The main contributions of this article are as follows. First, we introduce a novel model that characterizes the intrinsic property of full-view coverage in camera sensor networks. Second, we propose an efficient method to deterministically verify if a monitored field can be full-view covered by any given set of camera sensors. Third, we estimate the number of sensors needed for full-view coverage in a random deployment. Fourth, we obtain a sufficient and necessary condition on the sensor density needed for full-view coverage in a triangle lattice-based deployment. It is shown that the density required in this deployment pattern is no more than a factor of that needed in any other deployment. Fifth, we propose new models for weak and strong barrier coverage in camera sensor networks. Finally, under the two proposed barrier coverage models, novel solutions are presented to solve the coverage verification problems.

The rest of this article is organized as follows. Section 2 introduces the full-view coverage model. Section 3 gives the detailed description of full-view coverage detection for a given deployed camera sensor network. Section 4 shows the density estimation for full-view coverage in a random deployment. Section 5 presents the density calculation result for full-view coverage in a triangular lattice deployment pattern. Section 6 introduces the new weak coverage model and presents techniques to solve the weak barrier coverage verification problem. Section 7 proposes the new strong coverage model as well as solutions to the strong barrier coverage verification problem. Section 8 shows the evaluation results. The related work is reviewed in Section 9 and the article is concluded in Section 10.

2. NOTATIONS AND FULL-VIEW COVERAGE MODEL

Camera sensors[1] are deployed to monitor a bounded region A (target field). Each sensor S_i has a sensing range r, a field-of-view (FoV) angle φ, and an orientation vector $\vec{f_i}$, which together define the sensing sector (Figure 3(a)). We use S_i to denote the ith sensor. Without ambiguity, S_i also denotes the sensor's position. For any two points U, V, let $\|UV\|$ denote the (Euclidean) distance between them. For any two vectors $\overrightarrow{v_1}$ and $\overrightarrow{v_2}$, let $\alpha(\overrightarrow{v_1}, \overrightarrow{v_2})$ denote the angle between them, which ranges from 0 to π. A point

[1]We may use cameras or sensors for short throughout the article.

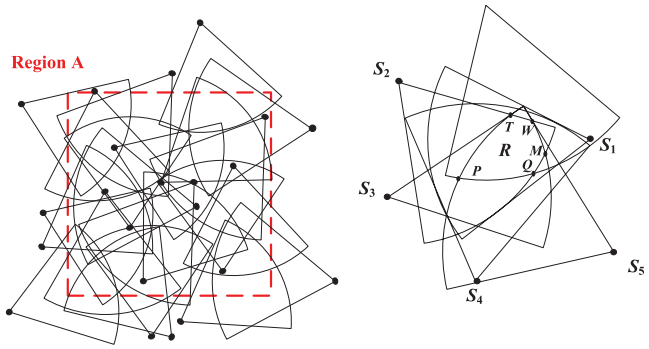

Fig. 4. (a) An example of a camera sensor network; how do we know if A is full-view covered? (b) A sub-region R whose boundary consists of five segments: $\overset{\frown}{TP}$, $\overset{\frown}{PQ}$, $\overset{\frown}{QM}$, $\overset{\frown}{MW}$, and $\overline{WT}$.

P is covered by a sensor S_i if P is in the sensing sector of S_i, that is, $\|PS_i\| < r$ and[2] $\alpha(\overrightarrow{f_i}, \overrightarrow{S_jP}) < \varphi/2$, where $\overrightarrow{S_jP}$ is the vector from S_j to P.

Definition 2.1 (*Full-View Coverage*). A point P is full-view covered if for any vector $\vec{d}$ (the facing direction), there is a sensor S_i, such that P is covered by S_i and $\alpha(\vec{d}, \overrightarrow{PS_i}) \leq \theta$ (Figure 3(b)). Here θ ($\in [0, \pi/2)$) is a predefined parameter which is called the *effective angle*. A region is full-view covered if every point in it is full-view covered.

In the preceding definition, $\overrightarrow{PS_i}$ represents the viewing direction[3] of camera S_i on object P. Also for notations, a vector $\vec{v}$ can be represented by an angle in $[0, 2\pi)$ with 0 degree indicating the vector pointing to the straight right, and vice versa. The angle is denoted by $arg(\vec{v})$ and always calculated by using arithmetic modulo 2π. For any angle $\alpha \in [0, 2\pi)$, the notation $vec(\alpha)$ represents the corresponding vector. For example, $vec(\frac{\pi}{2})$ represents the vector pointing upwards. We may use the notations of angle and vector interchangeably if no confusion is involved. And if we say a vector $\vec{v}$ falls into an interval $[\alpha_1, \alpha_2]$, we mean $\alpha_1 \leq arg(\vec{v}) \leq \alpha_2$.

3. FULL-VIEW COVERAGE DETECTION

In this section, we propose an efficient method to verify if the monitored region is full-view covered by a set of deployed camera sensors.

3.1. Method Overview

Given a set of deployed sensors, region A can be partitioned into subregions, where each subregion is defined to be a set of points covered by the same set of sensors. The boundary of each subregion consists of either segments of lines or arcs which are either part of the perimeter of the sensing sectors covering the subregion or part of A's boundary. For example, in Figure 4(b), subregion R is covered by five sensors and bounded by five segments: $\overset{\frown}{TP}$, $\overset{\frown}{PQ}$, $\overset{\frown}{QM}$, $\overset{\frown}{MW}$, and $\overline{WT}$.

We first show that the whole region is full-view covered if and only if the boundary of each subregion is full-view covered (Lemma 3.1). Then the most tricky part is to determine if every point on a boundary segment is full-view covered, as there are still an infinite number of positions to consider, and the sensor's viewing direction vary from

[2]For ease of analysis, we use $<$ instead of $\leq$, although it is not a necessary assumption.
[3]Intuitively, the viewing direction is from the camera to the object. We use the reverse to simplify analysis.

one position to another. To this end, we first show an equivalent condition on full-view coverage (Lemma 3.2), and then propose a novel method based on geometrical properties of the circumscribed circle and the inscribed angle (Lemma 3.3). The intuition is that if a point is full-view covered, there must be a set of sensors around it and the angle between the viewing directions of any two adjacent sensors is no more than 2θ. For any two sensors, we actually identify the area (called safe region) in which, for any point, the angle between the two sensors' viewing directions is no more than 2θ. Then we solve the detection problem by checking if the segment is contained in the safe region of every two adjacent sensors.

3.2. Detection Method

We need to verify if the condition in Definition 2.1 holds for every point in A. Actually we only need to verify if it holds on the boundary of every sub-region in A.

LEMMA 3.1 (BOUNDARY CONDITION). *The region A is full-view covered if and only if the boundary of every sub-region is full-view covered by the given set of sensors.*

PROOF. The "only if" part is obvious. We only need to show the "if" part, that is, for a given subregion R, if R's boundary segments are all full-view covered, then R is full-view covered.

Suppose there is an interior point $V \in R$ and a vector $\vec{d}$, such that for any sensor S_i with $\|VS_i\| < r$, $\alpha(\vec{d}, \vec{VS_i}) > \theta$. Now consider the intersection point of $\vec{d}$ and R's boundary, which is denoted by X (Figure 5). We claim that X is not full-view covered. In fact, consider a vector $\vec{d'}$ which is parallel to $\vec{d}$ and originates from X. If X is full-view covered, then there must be a sensor S_j such that $\|XS_j\| < r$, $\alpha(\vec{d'}, \vec{XS_j}) \leq \theta$. Clearly, S_j also covers V. Furthermore, we have $\alpha(\vec{d}, \vec{VS_i}) \leq \alpha(\vec{d'}, \vec{XS_j}) \leq \theta$, which is a contradiction. Therefore any interior point of R is full-view covered if the boundary is full-view covered. The claim is proved. □

Given a segment $\overline{PQ}$ on the boundary of a subregion R, where P and Q are the two end points of the segment, we show a way to determine if every point on the segment is full-view covered. Note that every point on $\overline{PQ}$ is covered by the same set of sensors. For any point $V \in \overline{PQ}$, we can construct a *circular list* of these sensors regarding their viewing direction on V as follows (Figure 6). Initially, the list is empty. We begin with any vector $\overrightarrow{VS_i}$ and place it into the list first. Then we rotate $\overrightarrow{VS_i}$ around V in the counterclockwise direction until it becomes parallel to the next vector $\overrightarrow{VS_j}$. Then we place $\overrightarrow{VS_j}$ into the list, right after $\overrightarrow{VS_i}$. We continue rotating and placing vectors sequentially into the list until we see the first vector again. Then the list is completed. We denote the list by $CL_V = \{\overrightarrow{VS_{V_1}}, \ldots, \overrightarrow{VS_{V_k}}\}$, where k is the number of sensors covering $\overline{PQ}$. Then the condition in Definition 2.1 is equivalent to the following.

LEMMA 3.2. *A given point V is full-view covered if and only if for CL_V constructed as previously, the rotation angle from $\overrightarrow{VS_{V_i}}$ to $\overrightarrow{VS_{V_{i+1}}}$ is less than or equal to 2θ for any $1 \leq i \leq k$, where $V_{k+1} = V_1$.*

PROOF. Suppose the condition holds. Then for any $\vec{d}$, there are two sensor S_{V_i} and $S_{V_{i+1}}$ such that either the rotation angle from $\overrightarrow{VS_i}$ to $\vec{d}$ or the angle from $\vec{d}$ to $\overrightarrow{VS_{V_{i+1}}}$ is less than or equal to θ. Thus V is full-view covered.

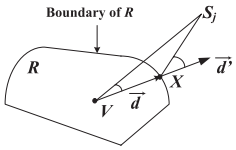

Fig. 5. Boundary condition.

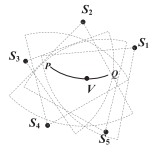

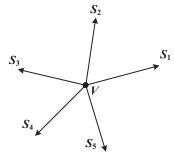

Fig. 6. The circular list of V.

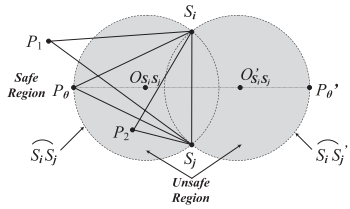

Fig. 7. The safe and unsafe region of S_i and S_j.

If V is full-view covered but the rotation angle from $\overrightarrow{VS_{V_i}}$ to $\overrightarrow{VS_{V_{i+1}}}$ is larger than 2θ for some i, then consider vector $\vec{d}$ along the bisector of the angle. The angle between either $\overrightarrow{VS_{V_i}}$ or $\overrightarrow{VS_{V_{i+1}}}$ and d is larger than θ. Therefore the statement is true. □

We need to determine if this condition holds for any $V \in \overline{PQ}$. To this end, we introduce the concept of safe region. For any two sensors S_i and S_j, we define the *safe region* to be the area in which for any point V, $\alpha(\overrightarrow{VS_i}, \overrightarrow{VS_j}) \leq 2\theta$; and define the *unsafe region* to be the area in which for any point V, $\alpha(\overrightarrow{VS_i}, \overrightarrow{VS_j}) > 2\theta$ (Figure 7). The following lemma shows an efficient method to identify the two regions.

LEMMA 3.3. *Given S_i and S_j, there are two arcs $\widehat{S_iS_j}$ and $\widehat{S_iS_j}'$ which connect S_i and S_j and are symmetrical with respect to line S_iS_j, such that the unsafe region is the enclosed region bounded by the arcs and the safe region is the open region outside the unsafe region.*

PROOF. We prove the lemma by showing how to find the two arcs. First we can find two different points P_θ and P'_θ on the perpendicular bisector of segment $\overline{S_iS_j}$, such that $\angle S_iP_\theta S_j = \angle S_iP'_\theta S_j = 2\theta$ and they are on different sides of S_iS_j. Without loss of generality, let P_θ be on the left side and P'_θ be on the right side (Figure 7).

We draw the circumscribed circles of triangle $\triangle S_iP_\theta S_j$ and $\triangle S_iP'_\theta S_j$. Denote the centers of the circles by $O_{S_iS_j}$ and $O'_{S_iS_j}$, and the radius (which is the same for both) by r_{safe}. Then arc $\widehat{S_iS_j}$ is the portion of the perimeter of $\odot O_{S_iS_j}$ on the left side and $\widehat{S_iS_j}'$ is the portion of $\odot O'_{S_iS_j}$ on the right.

In fact, for any circle and a fixed chord (defined here by $\overline{S_iS_j}$) of the circle, all inscribed angles with two endpoints at the ends of the chord are either equal or supplementary to each other. Specifically, they are equal if the third points of the angles are on the same side of the chord. Furthermore, for a given point P_θ on the perimeter of the circle and another point P on the same side of line S_iS_j as P_θ, if P is outside the circle ($\|PO_{S_iS_j}\| > r_{safe}$), then $\angle S_iPS_j < \angle S_iP_\theta S_j$; if P is inside the circle ($\|PO_{S_iS_j}\| < r_{safe}$), then $\angle S_iPS_j > \angle S_iP_\theta S_j$. The proof of this property can be found in any textbook on Euclidean Geometry and hence omitted here. □

Now we can give a necessary and sufficient condition for $\overline{PQ}$ to be full-view covered under some constraint.

THEOREM 3.4. *Suppose for every point $V \in \overline{PQ}$, the circular list $CL_V = \{VS_{V_1}, \ldots, VS_{V_k}\}$ is the same (in a circular way/order). Then $\overline{PQ}$ is full-view covered if and only if it is within the polygon bounded by $\{\overline{S_{V_i}S_{V_{i+1}}}, 1 \leq i \leq k\}$ and for any*

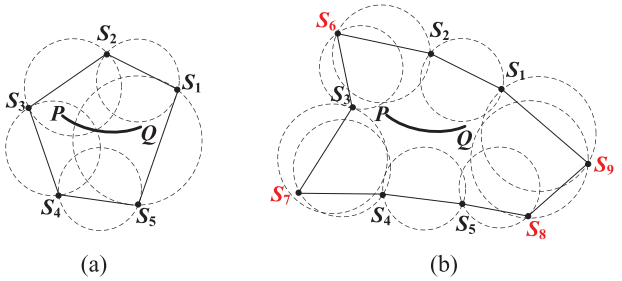

Fig. 8. (a) $\overline{PQ}$ is not full-view covered; (b) $\overline{PQ}$ is full-view covered.

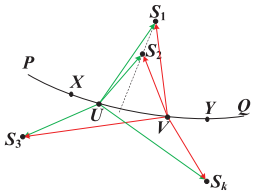

Fig. 9. The circular lists for U, V are different: $CL_V = \{S_1, S_2, \ldots, S_k\}$ but $CL_U = \{S_2, S_1, \ldots, S_k\}$.

$1 \le i \le k$, the unsafe region of S_{V_i} and $S_{V_{i+1}}$ does not intersect with $\overline{PQ}$, where V_{k+1} denotes V_1.

PROOF. This is a direct result from Lemmas 3.2 and 3.3. □

We use an example to illustrate our idea (Figure 8). In Figure 8(a), the distribution of the sensors is the same as that in Figure 6. We draw the boundaries of the unsafe regions for the five pairs of neighboring sensors (indicated by dotted circles) as in Lemma 3.3, and check if they intersect with $\overline{PQ}$ (in computation, this can be done by comparing the distance between the circle's center to $\overline{PQ}$ with the circle's radius). As can be seen, $\overline{PQ}$ intersects with the unsafe regions of S_2S_3, S_3S_4, and S_5S_1, and hence it is not full-view covered. Figure 8(b) shows the case when there are four other sensors S_6, S_7, S_8, and S_9 covering $\overline{PQ}$. In this case, $\overline{PQ}$ can be full-view covered as no unsafe region intersects with it.

However, the circular list CL_V may not be the same for every point $V \in \overline{PQ}$. For example, in Figure 9, S_1 is prior to S_2 in V's list, but S_2 is prior to S_1 in U's list. To resolve this issue, we partition $\overline{PQ}$ into subsegments. For $1 \le i \le k-1$ and $i+1 \le j \le k$, if the line S_iS_j intersects with $\overline{PQ}$, we mark the intersection point on $\overline{PQ}$. Then $\overline{PQ}$ is partitioned into subsegments defined by every two adjacent marked points (including P and Q). Since there are at most $k(k-1)$ intersection points, the total number of subsegments is $O(k^2)$. Moreover, for a specific subsegment $\overline{XY}$, where X and Y are two adjacent marked points, all points on it have the same circular list of the sensors. Actually, if this is not true, there must be two points $U, V \in \overline{XY}$, and two sensors $S_1, S_2 \in S_R$, such that S_1 comes before S_2 in V's list but S_2 is before S_1 in U's list and there are no other sensors between them (Figure 9). Then line S_1S_2 must have an intersection point with $\overline{PQ}$, between X and Y, which is a contradiction to the fact that X and Y are adjacent intersection points.

Now we have a complete procedure for full-view coverage detection on a given segment of a subregion's boundary. We can further apply this on all segments in A. For an estimation of the total running time, the whole region can be considered as a planar

graph, where the vertices are the intersection points of sensing sectors and edges are the segments. As any two sensing sectors can have $O(1)$ intersection points on the perimeters, the number of vertices is $O(N^2)$, where N is the total number of sensors. This further implies the total number of segments is $O(N^4)$. Our detection method requires $O(k^2)$ time on each segment, where k ($\leq N$) is the number of sensors covering this segment. Therefore the total running time must be a polynomial function of N.

4. SENSOR DENSITY ESTIMATION FOR FULL-VIEW COVERAGE IN RANDOM DEPLOYMENT

In this section, we derive an estimation on the lower bound of the probability that a region is full-view covered by a given number of randomly distributed sensors. With this result, we can estimate the sensor density needed to achieve full-view coverage with any given probability (e.g., 0.99).

4.1. Technique Overview

Consider a random uniform distribution of N sensors in a square region A. Without loss of generality, we assume A is of unit area. Given r, φ, and θ, we estimate the probability that A is full-view covered. Generally, if sensors are deployed in a bounded region, the area very close to the boundary is likely to have fewer sensors than the interior area, and hence less likely to be covered as required. A common method for avoiding this boundary effect is to deploy the sensors in a slightly larger region A', for example, enlarging the side length of A from d to $d + r$. The difference is negligible if A is sufficiently large. We can also make the analysis clean by assuming the sensor's coverage reflects at the boundary; that is, for each sensor S with distance less than r to a boundary, we assume there is another sensor outside the boundary at the position symmetrical to S with respect to the boundary. In the following analysis, we assume the boundary effect is negligible.

First we approximate the continuous region by discrete grid points. We show that if the grids are sufficiently dense and are all full-view covered by a set of sensors with (r', φ', θ'), where $r' = r - \Delta r$, $\varphi' = \varphi - \Delta\varphi$, and $\theta' = \theta - \Delta\theta$ for any given $(\Delta r, \Delta\varphi, \Delta\theta)$, then the whole region is full-view covered by the same set of sensors with (r, φ, θ). Then we give a lower bound of the probability that all grid points are full-view covered. Based on this, we obtain a lower bound of the probability that A is full-view covered.

In the following analysis, we first assume $\varphi = 2\pi$. This will give the essence of our method. Note that the major challenge of full-view coverage is due to the introduction of θ, not φ. It should be clear that full-view coverage with $\varphi = 2\pi$ is completely different from the traditional disk coverage. In practice, $\varphi = 2\pi$ can be considered as the case that each node is a bundle of multiple cameras, facing to different directions to form a panoramic view. A camera that rotates around with negligible rotation time can also be considered as in this case. After that we extend the analysis to any $0 < \varphi < 2\pi$.

4.2. Probability Estimation for $\varphi = 2\pi$

We use triangle lattices as the grids, although any other grid patterns may also suffice. Grid points are the vertices of equilateral triangles with side length l. Each grid point P has six neighbors with distance l from it (Figure 10). They are called P's one-hop neighbors. Given A's area fixed to be unit, the choice of l depends on $(\Delta r, \Delta\theta)$.

LEMMA 4.1. *Given $(\Delta r, \Delta\theta)$, if $l \leq l_0(\Delta r, \Delta\theta)$, for any point $V \in A$ and any vector $\vec{d}$ from V, there is a grid point P such that $\|VP\| \leq \Delta r$ and $\alpha(\vec{d}, \overrightarrow{VP}) \leq \Delta\theta$. Here $l_0(\Delta r, \Delta\theta) = \frac{2\Delta r}{\sqrt{3}+\cot\Delta\theta}$.*

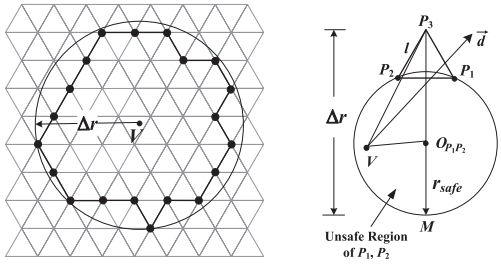

(a) (b)

Fig. 10. (a) Black dots are edge points of V; (b) if V is in the unsafe region of P_1, P_2, P_3 is an edge point.

PROOF. Consider the set of all the grid points P with $\|VP\| \leq \Delta r$, which is denoted by $GP_V(\Delta r)$. Define an edge point to be a grid point $P \in GP_V(\Delta r)$ such that P has an one-hop neighbor not in $GP_V(\Delta r)$ and a one-hop neighbor in $GP_V(\Delta r)$.

All the edge points and the line segments connecting them form a polygon just inside the circle centered at V with radius Δr (Figure 10(a)). Suppose the intersection point of vector $\vec{d}$ and the polygon's boundary is between two neighboring edge points P_1, P_2. We claim $\alpha(d, VP_1) + \alpha(d, VP_2) \leq 2\theta$, which will prove the lemma.

Suppose the claim is incorrect. Then from Lemma 3.3, V is in the unsafe region of P_1, P_2, which means $\|VO_{P_1P_2}\| < r_{safe}$, where $O_{P_1P_2}$ is the center of the circle defining the unsafe region (Figure 10(b)). From trigonometry knowledge, we get $r_{safe} = \frac{l}{2\sin(2\Delta\theta)}$. So

$$\|VO_{P_1P_2}\| < \frac{l}{2\sin(2\Delta\theta)}.$$

Consider the triangles with P_1P_2 as one side and a third vertex P_3. P_3 is either on the near side of P_1P_2 and closer from V or on the far side of P_1P_2 and further from V. Consider the case when P_1 is on the far side. Then $\|VP_3\| > \Delta r$ (since if else, either P_1 or P_2 is not edge point).

On the other hand,

$$\|P_3O_{P_1P_2}\| = r_{safe} \cdot \cos 2\theta + \frac{\sqrt{3}}{2}l = \frac{l}{2}(\cot 2\Delta\theta + \sqrt{3}).$$

If l is as in the lemma, from triangle inequality,

$$\|VP_3\| \leq \|VO_{P_1P_2}\| + \|P_3O_{P_1P_2}\| < \Delta r.$$

This is a contradiction. Thus the claim is proved. □

Based on this result, we have the following condition regarding the whole region's coverage.

LEMMA 4.2. *Suppose $\varphi = 2\pi$ and all grid points are full-view covered by a set of sensors with $r' = r - \Delta r$ and $\theta' = \theta - \Delta\theta$ for some given $(\Delta r, \Delta\theta)$. If $l \leq l_0(\Delta r, \Delta\theta)$ as indicated in Lemma 4.1, then any point $V \in A$ is full-view covered by the same set of sensors with (r, θ).*

PROOF. We need to prove that for any point $V \in A$ and any vector $\vec{d}$, there is a sensor S_i such that $\|S_iV\| < r$ and $\alpha(\overrightarrow{VS_i}, \vec{d}) \leq \theta$.

Suppose P is the grid point found in Lemma 4.1. Since P is full-view covered, there is a sensor S_j such that $\|PS_j\| < r'$ and $\alpha(\overrightarrow{VP}, \overrightarrow{PS_j}) \leq \theta'$ (Figure 11(a)). From triangle

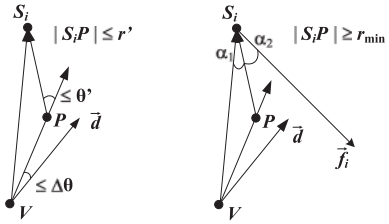

Fig. 11. Grid point property: (a) there is no constraint on the distance between P and S_i (Lemma 4.2); (b) there is a lower bound r_{min} on the distance between P and S_i (Lemma 4.5).

inequality,

$$\|VS_j\| \le \|VP\| + \|PS_j\| < \Delta r + r' = r.$$

Thus V is covered by S_j, and furthermore,

$$\alpha(\vec{d}, \overrightarrow{VS_j}) \le \alpha(\vec{d}, \overrightarrow{VP}) + \alpha(\overrightarrow{VP}, \overrightarrow{VS_j}) \le \Delta\theta + \theta' = \theta.$$

Thus V is full-view covered by the sensors with (r, θ). □

For any point $V \in A$, let C_V denotes the event that V is full-view covered.

LEMMA 4.3. *Suppose $\varphi = 2\pi$. Given N sensors with (r', θ') uniformly distributed in A, the probability that a given point V is full-view covered is*

$$Pr(N, r', \theta') = Pr[C_V] = \sum_{k=\frac{\pi}{\theta'}}^{N} \binom{N}{k} p^k (1-p)^{N-k} f(k, \theta'),$$

where π/θ' is the abbreviation for $\lfloor \pi/\theta' \rfloor$, $p = \pi r'^2$ and

$$f(k, \theta') = \sum_{j=0}^{\frac{\pi}{\theta'}} \binom{k}{j} (-1)^j \left(1 - j\frac{\theta'}{\pi}\right)^{k-1}.$$

PROOF. For a uniformly distributed sensor S_i, the probability that it is within distance r' from V is $p = \pi r'^2$ and the probability that exactly k sensors are within r' to V is $\sum_{k=\frac{\pi}{\theta'}}^{N} \binom{N}{k} p^k (1-p)^{N-k}$.

Consider the distribution of the sensor within the disk, since the sensor is uniformly distributed in A, its distribution is also uniform if restricted to the disk area within distance r' to V. Furthermore, for each sensor S_i within the disk, consider its projection P_i on the perimeter of the circle centered at V with radius r'. It is the intersection point of vector $\overrightarrow{VS_i}$ and the circle. If we consider P_i's position on the circle, it is also uniformly distributed. From Lemma 3.2, given k sensors within distance r' from V (and hence able to cover V), V is full-view covered if and only if the angle between any two adjacent vectors is no greater than 2θ. This is equivalent to the event that the perimeter of a circle with unit length is covered by k uniformly distributed arc segments with length θ'/π (Figure 12). The latter probability is given by $f(k, \theta')$, which is shown in Solomon [1978]. Therefore we have the probability shown in the lemma. □

From Lemmas 4.2 and 4.3, we obtain a lower bound on the probability for region A to be full-view covered.

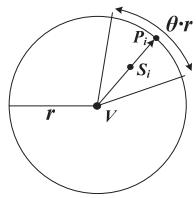

Fig. 12. S_i's coverage range is projected as an arc on a unit circle.

THEOREM 4.4. *Given r, θ and $\varphi = 2\pi$, the probability that region A is full-view covered by N uniformly distributed sensors is lower bounded by $Pr(N, \frac{\sqrt{N}-1}{\sqrt{N}}r, \frac{\sqrt{N}-1}{\sqrt{N}}\theta)^M$, where $Pr(N, x, y)$ is given by Lemma 4.3, $M = \lceil \frac{8}{\sqrt{3}} l_0^{-2} \rceil$ and $l_0 = l_0(\frac{r}{\sqrt{N}}, \frac{\theta}{\sqrt{N}})$ is given by Lemma 4.1.*

PROOF. From Janson's Inequality [Alon and Spencer 2000] and Lemma 4.3, the probability that all grid points are full-view covered by N sensors with $r' = \frac{\sqrt{N}-1}{\sqrt{N}}r$ and $\theta' = \frac{\sqrt{N}-1}{\sqrt{N}}\theta$ is no less than $Pr(N, r', \theta')^M$, where M is the number of grid points in a unit area. Then from Lemma 4.2, the whole area is full-view covered by sensors with $r = r' + \Delta r$ and $\theta = \theta' + \Delta\theta$, where $\Delta r = \frac{1}{\sqrt{N}}r$ and $\Delta\theta = \frac{1}{\sqrt{N}}\theta$, if the grid points are full-view covered by the same set of sensors with (r', θ'). Therefore we have the lower bound shown. □

4.3. Probability Estimation for $\varphi < 2\pi$

We use similar techniques as the preceding. Note that Lemmas 4.1 and 4.2 are the keys to the establishment of the preceding result. The rationale behind it is that if the grid points are sufficiently dense and all full-view covered, the whole region can be full-view covered if we slightly enlarge the sensor's radius and the effective angle. However, we assumed $\varphi = 2\pi$ there, which means any point V within Δr to a grid point P is also covered by the sensors that cover P, and hence makes the analysis clean. If $\varphi < 2\pi$, the sensor covering P may not cover V due to the sensor's orientation, no matter how close they might be to each other. A natural solution is to expand φ' to φ. However, it is difficult to guarantee a bound on how large it should increase to (α_1 in Figure 11(b)), and if we can not reasonably bound this value, the error of the estimation would be large. To overcome this difficulty, we require the grid points to be full-view covered by sensors which are at least certain distance (a tiny lower bound) away from it. Then we can establish similar results as in Lemmas 4.1 and 4.2.

LEMMA 4.5. *Suppose each grid point can be full-view covered by sensors that are at least r_{min} distance away and with parameters $r' = r - \Delta r$, $\theta' = \theta - \Delta\theta$, and FoV angle $\varphi' = \varphi - \Delta\varphi$, for some predefined $(\Delta r, \Delta\theta, \Delta\varphi)$. If $l \le l(\Delta r, \Delta\theta, \Delta\varphi)$, then any point in A is full-view covered by the same set of sensors with (r, θ, φ). Here $l(\Delta r, \Delta\theta, \Delta\varphi) = \frac{\min\{2\Delta r, \Delta\varphi \cdot r_{min}\}}{\sqrt{3}+\cot\Delta\theta}$.*

PROOF. We need to show that for any $V \in A$ and any facing direction (vector $\vec{d}$), there is a sensor S_i such that $\|VS_i\| < r$, $\alpha(\overrightarrow{S_iV}, \overrightarrow{f_i}) \le \varphi/2$ and $\alpha(\overrightarrow{VS_i}, \vec{d}) \le \theta$, where $\overrightarrow{f_i}$ is the orientation vector of S_i. We first observe that if l is as indicated as preceding, it also satisfies the condition in Lemma 4.1. So there must be a grid point P such that $\|VP\| \le \min\{\Delta r, \Delta\varphi \cdot r_{min}/2\}$ and $\alpha(\vec{d}, \overrightarrow{VP}) \le \Delta\theta$. Moreover, among the sensors that cover

P, there must be a sensor S_i such that $\|VS_i\| < r$ and $\alpha(\overrightarrow{VS_i}, \vec{d}) \leq \theta$. We only need to show that $\alpha(\overrightarrow{S_iV}, \overrightarrow{f_i}) \leq \varphi/2$.

Note that $\alpha(\overrightarrow{S_iV}, \overrightarrow{f_i}) \leq \alpha_1 + \alpha_2$, where $\alpha_1 = \alpha(\overrightarrow{S_iV}, \overrightarrow{S_iP})$ and $\alpha_2 = \alpha(\overrightarrow{S_iP}, \overrightarrow{f_i})$ (Figure 11(b)). As P is covered by S_i, $\alpha_2 \leq \varphi'/2$. From trigonometry knowledge, we know $\alpha_1 \leq \tan\alpha_1 = \frac{\|VP\|\sin\beta}{\|VP\|\cos\beta + \|PS_i\|}$, where $\beta = \alpha(\overrightarrow{PS_i}, \overrightarrow{VP})$. Notice that $\|VP\| \leq \Delta\varphi \cdot r_{min}/2$, $\|PS_i\| \geq r_{min}$ and $\sin\beta \leq 1$. Therefore, $\alpha_1 \leq \Delta\varphi/2$, and hence $\alpha(\overrightarrow{S_iV}, \overrightarrow{f_i}) \leq \varphi'/2 + \Delta\varphi/2 \leq \varphi/2$. □

For any point $V \in A$, let $C_V^{r_{min}}$ denote the event that V is full-view covered by sensors which are at least $r_{min}(< r)$ distance away.

LEMMA 4.6. *Given N sensors with (r', θ', φ') uniformly distributed in region A, the probability for a given point V to be full-view covered by sensors at least $r_{min}(< r')$ away is*

$$\begin{aligned} Pr(N, r_{min}, r', \theta', \varphi') &= Pr\left[C_V^{r_{min}}\right] \\ &= \sum_{s=\frac{\pi}{\theta'}}^{N} \binom{N}{s} p^s (1-p)^{N-s} \sum_{k=\frac{\pi}{\theta'}}^{s} \binom{s}{k} q^k (1-q)^{s-k} f(k, \theta'), \end{aligned}$$

where π/θ' is the abbreviation for $\lfloor \pi/\theta' \rfloor$, $p = \pi(r'^2 - r_{min}^2)$, $q = \varphi'/2\pi$, and $f(k, \theta')$ is as in Lemma 4.3.

PROOF. First note that given a sensor S_i with $r_{min} \leq \|VS_i\| \leq r'$, since its orientation vector is uniformly distributed in $[0, 2\pi)$, the probability that V is covered by S_i is q. Also note that the probability that a sensor falls into the closed strip, with r' as outer radius and r_{min} as inner radius, is p. The meaning of $f(k, \theta')$ is the same as in Lemma 4.3. By combining these together, we have $Pr[C_V^{r_{min}}]$ as previously shown. □

Now we can give a lower bound of the probability that A is full-view covered.

THEOREM 4.7. *Given (r, θ, φ), the probability that region A is full-view covered by N uniformly distributed sensors is lower bounded by $Pr(N, \frac{r}{\sqrt{N}}, \frac{\sqrt{N}-1}{\sqrt{N}}r, \frac{\sqrt{N}-1}{\sqrt{N}}\theta, \frac{\sqrt{N}-1}{\sqrt{N}}\varphi)^M$, where $Pr(N, w, x, y, z)$ is given by Lemma 4.6, $M = \lceil \frac{8}{\sqrt{3}} l^{-2} \rceil$ and $l = l(\frac{r}{\sqrt{N}}, \frac{\theta}{\sqrt{N}}, \frac{\varphi}{\sqrt{N}})$ is given by Lemma 4.5.*

PROOF. From Lemmas 4.5 and 4.6, this can be proved by following the same argument as in Theorem 4.4. □

5. DENSITY ESTIMATION FOR FULL-VIEW COVERAGE IN DETERMINISTIC DEPLOYMENT

Deterministic deployment is the best way to achieve full-view coverage in a controlled environment, for example, in indoor surveillance where camera sensors can be placed at any place as required. In the traditional disk model, triangle lattice-based deployment is proved to be optimal in terms of sensor density [Kershner 1939]. In this section, we construct a deployment pattern for full-view coverage based on the triangle lattice. We show a necessary and sufficient condition on the grid length such that the whole area can be full-view covered. Based on that, we derive an estimation on the sensor density needed for full-view coverage in the triangle lattice based deployment and show that it is at most a factor from the optimal deployment pattern.

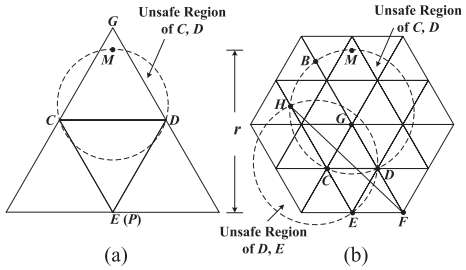

Fig. 13. Necessary condition for triangle lattice: (a) $\theta \geq \pi/6$; (b) $\theta < \pi/6$.

5.1. Triangle Lattice

The triangle lattice is constructed as follows. First we place $\lceil 2\pi/\varphi \rceil$ sensors together on a single point and let them face different directions to form a single node with $\varphi = 2\pi$. Then we place the sensor nodes on the vertices of the equilateral triangles with grid length l. Region A has unit area and it is assumed to be sufficiently large compared with r and hence we ignore the boundary effect in deployment.

5.2. Density Estimation for Triangle Lattice Based Deployment

The grid length l of the triangle is critical. If it is too large, there will be points not full-view covered. If it is too small, the deployment density and hence the cost may be too high. Given the sensor radius r and the effective angle θ, we want to calculate the best l such that every point in A is full-view covered.

Actually if we replace $(\Delta r, \Delta\theta)$ by (r, θ) in Lemma 4.1, we immediately have a sufficient condition on l.

LEMMA 5.1. *Suppose sensors are deployed on the vertices of the triangle lattices with grid length l. Given (r, θ), if $l = l(r, \theta) = \frac{2r}{\sqrt{3}+\cot\theta}$, then every point in A is full-view covered.*

PROOF. This is a direct result from Lemma 4.1. □

In fact, this is also a necessary condition for full-view coverage in the triangle lattice based deployment.

LEMMA 5.2. *If region A is full-view covered, the grid length should be no smaller than $l = l(r, \theta) = \frac{2r}{\sqrt{3}+\cot\theta}$.*

PROOF. There are two cases: $\theta \geq \pi/6$ and $\theta < \pi/6$. If $\theta \geq \pi/6$, consider the situation in Figure 13(a). M is the intersection point of EG and the boundary of the unsafe region of C, D, which is a portion of the circle centered at $O_{C,D}$. Let V be a point on the segment EM and with distance $\epsilon(> 0)$ to M. Let $r' = \|EV\|$. Since V is in the unsafe region of C, D, which means $\angle CVD > 2\theta$, there must be a grid point P such that either $\angle CVP < 2\theta$ or $\angle DVP < 2\theta$ and P can cover V. This can only happen if $r \geq r'$ (and hence P is E), because if not, there would be no grid point between line VC and VD which can cover V. Let $\epsilon \to 0$ and hence $r \to r' = \|EM\|$, which implies the critical value of l.

If $\theta < \pi/6$, consider the situation in Figure 13(b). In this case, the boundary of the unsafe region of C, D intersects with line EC on H and intersects with line DG on B. First we notice that H is also the intersection point of the boundary of the unsafe region of E, D and line EC. In fact, if we denote this intersection point by H', then $\angle EH'D = 2\theta$ according to Lemma 3.3. Similarly, $\angle EHD$ also equals to 2θ. Since H and H' are on the same line, they are the same point. Then since HE is parallel to BD, $\|HB\| = \|DE\|$, which further equals to $\|CD\|$ and $\|CG\|$. Thus polygon $HCGB$ is

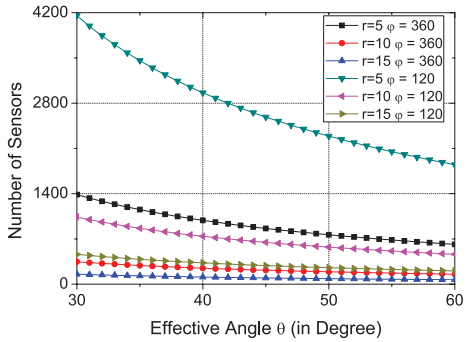

Fig. 14. Number of sensors needed in a triangular lattice-based deployment.

a parallelogram, which means $\|HC\| = \|BG\|$. From this, we know $\triangle HCF$ and $\triangle BGE$ are congruent triangles, which means $\|HF\| = \|BE\|$. By a similar argument as in the above case, we know that if r is smaller than $\|HF\|$, there is a point sufficiently close to H such that it is not full-view covered. Now consider the case when $\theta \to 0$. This implies $\|HF\| = \|BE\| \to \|BG\|$ and $\|BG\| \to \|EM\|(\to \infty)$, which further implies $\|HF\| = \|EM\|$ and hence we have the critical value of l. □

From the preceding critical value of l obtained, we calculate the required sensor density for the triangle lattice-based deployment. We compare it with other possible deployment patterns.

THEOREM 5.3. *Given (r, θ, φ), the sensor density for the triangle lattice-based deployment is $\frac{\pi}{\varphi|A_l|}$ which is no more than $\frac{\theta r^2}{2|A_l|}$ of the density required by any other deployment patterns for full-view coverage of region A. Here $|A_l| = \frac{\sqrt{3}r^2}{3+2\sqrt{3}\cot\theta+(\cot\theta)^2}$, which is the area of a equilateral triangle with side length l given in Lemma 5.2.*

PROOF. First, from Lemma 5.1 we know l and hence the area of each triangle with side length l, which is exactly $|A_l|$ shown previously. Then note that each triangle has three vertices, and each vertex is the intersection point of six triangles. Thus the total number of grid points in a unit area region is $\frac{|A|}{|A_l|} \cdot \frac{3}{6} = \frac{1}{2|A_l|}$. Thus the total number of sensors needed is $\frac{2\pi}{\varphi} \cdot \frac{1}{2|A_l|} = \frac{\pi}{\varphi|A_l|}$.

On the other hand, for any deployment patterns, each point in A should be covered by at least π/θ sensors. Note that each sensor can only cover $\varphi r^2/2$ area of A, which is the area of the sensing sector. Thus the total number of sensor needed is at least $\frac{\pi/\theta}{\varphi r^2/2} = \frac{2\pi}{\theta\varphi r^2}$.

Finally, the ratio of the above two values yields the bound on the scaling factor in the theorem. □

Figure 14 is an illustration on the number of sensors needed for full-view coverage in an 100m × 100m field when triangular lattice-based deployment is used (θ is from $\frac{\pi}{6}$ to $\frac{\pi}{3}$, for $r = 5, 10, 15$ and $\varphi = \frac{2}{3}\pi, 2\pi$, respectively).

6. WEAK BARRIER COVERAGE IN CAMERA SENSOR NETWORKS

In traditional wireless sensor networks, two kinds of notations of barrier coverage have been identified: weak barrier coverage and strong barrier coverage [Kumar et al. 2005]. The situation is much more complicated in camera sensor networks. One factor to consider, as in existing models, is the object's path. The object can either take a

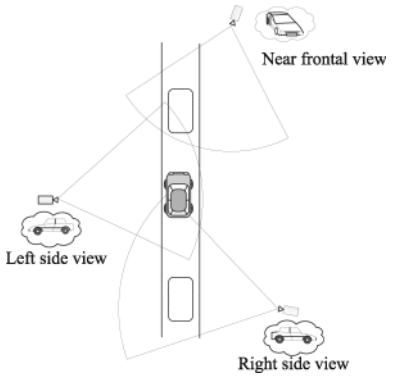

Fig. 15. Although there is no single point on the path where the vehicle is full-view covered, multiple views of the car body will be accumulated along the way.

shortest (i.e., along a straight line) or non-shortest path to cross the field. Another factor, which is unique to the camera sensor network, is where the object could face, or which aspect of the object we want to see.

In the following sections, we study the barrier coverage problem in camera sensor networks. We first consider the scenario when the object always takes the shortest path, that is, a straight line to cross the field. A new weak barrier coverage model is proposed. Then the weak barrier coverage verification problem is studied. The problem asks if the monitored field is under weak barrier coverage given a deployed camera sensor network. A series of procedures to verify the coverage will be introduced. Then in the next section, the assumption will be relaxed such that the object can take any possible path between the entrance and the exit and has more flexibility on choosing the facing direction. It is not difficult to see that the stronger the coverage is (or the more choices the object has), the more camera sensors are needed.

6.1. Weak Barrier Coverage of Camera Sensors

Consider the case when the object takes a shortest path to cross the field. In practice, we may want to observe the object from multiple aspects. One example can be found in an application to monitor vehicles crossing the field. One may require the frontal image of the vehicle that contains the plate information and the driver's face image to be observed. It is also likely for the application to ask for a side view so that the specific model of the vehicle can be identified. In these cases, a proper coverage should provide views all around the vehicle as it passes over the monitored field. Note that the purpose is not to provide a full-view coverage at one spot, but to accumulate multiple views along the way (Figure 15). Based on this, we develop a new weak barrier coverage model for camera sensor networks.

Consider a two-dimensional rectangular area A with one side being the entrance and another side being the exit. A camera sensor network $S = \{S_1, \ldots, S_n\}$ has been deployed to monitor A. The weak barrier coverage of the camera sensor network is defined as follows.

Definition 6.1. The monitored field A is said to be under weak barrier coverage by the deployed camera sensor network if for any object traveling from the entrance to the exit along any straight path, and for any predefined facing direction, there is a point P on the path such that P is coved by a camera sensor S_i, and the angle between $\vec{v}$ and $\overrightarrow{PS_i}$ is smaller than the effective angle θ.

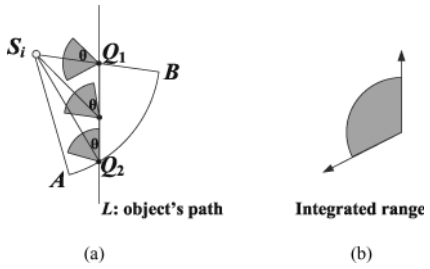

Fig. 16. The object's face can only be detected if it is within $\overline{Q_1Q_2}$ and faces to certain direction: (a) as it travels from Q_2 to Q_1, the range in which it will be detected will gradually shifts (the grey sectors); (b) the union of the range is the sum (integrated range) of facing direction where the object's face will be detected within $\overline{Q_1Q_2}$.

Note that in this definition and the rest of the article, we use the term "face" or "facing direction" to denote any aspect of the object that we are interested in. As before, it can be represented by an angle from 0 to 2π. With this definition, the problem considered here is defined as follows.

Definition 6.2 (*Weak Barrier Coverage Verification*). Given a rectangular field A to be monitored, and a network of camera sensors $S = \{S_1, \ldots, S_n\}$ with fixed sensing radius r and FoV angle φ but arbitrary locations and orientations, also given the effective angle $\theta \in [0, \frac{\pi}{2})$, the problem asks whether A is under weak barrier coverage by S.

The challenge to the problem comes from the requirement that an object needs to be covered from multiple views during the trip crossing the field. Unlike in classic coverage model where the coverage only depends on the distance between the traversing path and the sensor, the impact of each individual camera also depends on its viewing direction to the object, which changes continuously when the object moves.

6.2. Conversion into 2D Coverage Verification

The key is to map the preceding problem into a classic two-dimensional coverage problem, in which a predefined area is to be covered by a set of subareas and no direction issue is involved.

Given the rectangular area A to be monitored, consider a crossing path L and a camera S_i covering a portion of L. When an object P travels within the covered portion of L, its face (or any given aspect) will be detected by S_i, if its facing direction falls into the range $[arg(\vec{PS_i}) - \theta, arg(\vec{PS_i}) + \theta]$ (recall that $arg(\vec{v})$ is the angle representing the vector $\vec{v}$). Obviously, as P moves, this range will shift accordingly. There are two critical positions of P, which are the two intersection points of L and the boundary of S_i's sensing range (Figure 16). One of the points is closer to the exit, denoted by Q_1, and the other is closer to the entrance, denoted by Q_2.[4] Consider the case when L is to the right of S_i, as shown in Figure 16. Then as P travels from Q_2 to Q_1, its face will be detected if its facing direction is within

$$\begin{aligned} &(arg(\vec{Q_2S_i}) - \theta, arg(\vec{Q_1S_i}) + \theta), \text{ if } arg(\vec{Q_2S_i}) - \theta < arg(\vec{Q_1S_i}) + \theta; \\ &(arg(\vec{Q_2S_i}) - \theta, 2\pi) \cup [0, arg(\vec{Q_1S_i}) + \theta), \text{ otherwise.} \end{aligned} \tag{1}$$

Here the angle is calculated by using modulo 2π, which means if $arg(\vec{Q_2S_i}) - \theta \geq arg(\vec{Q_1S_i}) + \theta \geq 2\pi$, the actual interval will be from $2\pi + arg(\vec{Q_2S_i}) - \theta$ to 2π and then

[4]Note that if the distance between L and S_i is equal to r, then Q_1 and Q_2 are the same point.

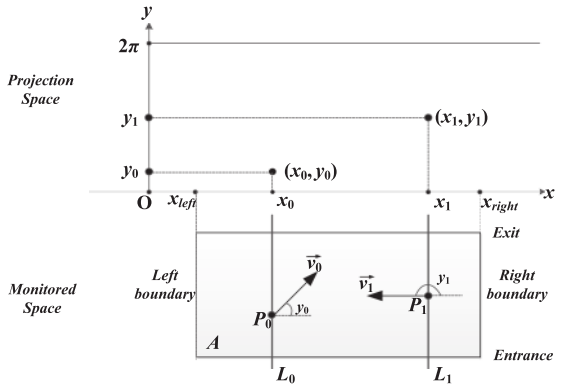

Fig. 17. In the monitored space, field A is to be covered by the camera sensors. A facing direction $\vec{v_i}$ with angle y_i at a particular point of a crossing path L_i, represented by $x = x_i$, is projected onto a point (x_i, y_i) in the projection space. If v_i is covered at some spot P_i on the path L_i, (x_i, y_i) is covered.

from 0 to $arg(\vec{Q_1S_i}) + \theta$. Similar expression can be obtained for the case when L is to the left of S_i.

To characterize the preceding relationship between L's position and the coverage, a 2D Cartesian coordinate system is used with the x axis parallel to A's width (horizontal) and the y axis perpendicular to the x axis (Figure 17). Any shortest path L across the field is mapped onto a point on the x axis. Let the leftmost path (i.e., the left boundary) be mapped onto $x = x_{left}$ and the rightmost path be mapped onto $x = x_{right}$.

In this coordinate system, the y axis indicates the facing direction, which means only the range $[0, 2\pi)$ will be considered. In this system, a point (x_0, y_0) is said to be covered (or marked covered) if the following is true: when the object travels along the path $x = x_0$ and faces to the direction y_0, its face is detected. In general, consider a path L corresponding to $x = x_L$. If the object's face is detected when its facing direction is within $[\alpha_1, \alpha_2]$, then all points with x coordinate equal to x_L and y coordinate within $[\alpha_1, \alpha_2]$ in the new coordinate system are marked covered.

To avoid confusion, the new coordinate system is referred to as the *projection space*, and the original space where the field A is defined is referred to as the *monitored space*. From the preceding description, it should be clear that a point (x, y) marked covered in the projection space has nothing to do with the coverage of the point (x, y) in the monitored space.

From Definition 6.2 and the preceding discussion, it is clear that the following lemma is true.

LEMMA 6.3. *The monitored field A is under weak barrier coverage if and only if in the projection space the following area*

$$A_{proj} = \{(x, y) : x \in (x_{left}, x_{right}), y \in [0, 2\pi)\} \tag{2}$$

is covered.[5]

6.3. Coverage of Individual Camera Sensor

For a given L and S_i, it is not difficult to find the set of points to be marked covered in the projection space. However, the number of paths to be considered in the monitored space is countless. An efficient way is needed to characterize the set of marked points in the projection space. In the following discussion, for each S_i, a mathematical expression

[5]We use open set for ease of presentation and to make the analysis clean, although it is not necessary.

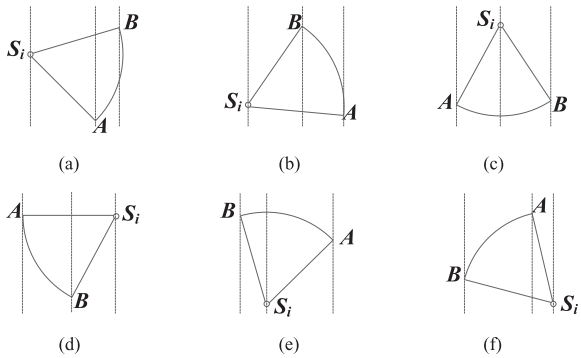

Fig. 18. There are six cases to consider in the computation of an individual camera's coverage impact.

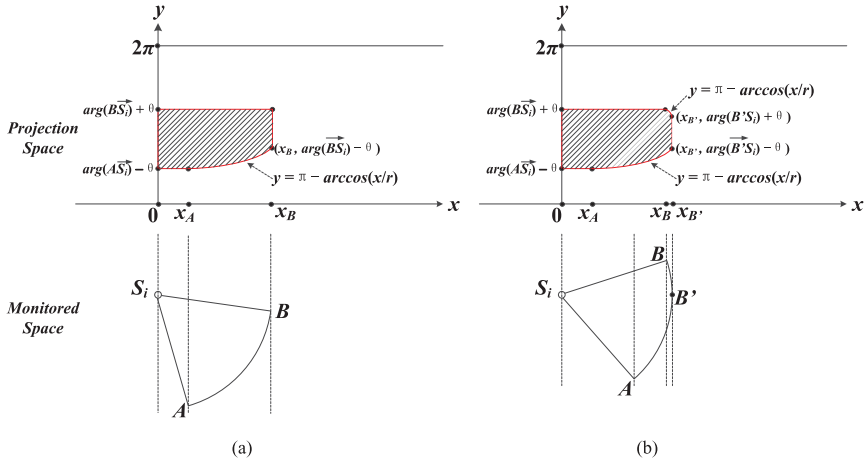

Fig. 19. The computation of an individual camera sensor's coverage: (a) vertex B is the rightmost point of S_i's sensing range; (b) another point B' that is on the $\widehat{AB}$ is the rightmost point of S_i's sensing range.

is obtained to describe the shape of the set of all points that are marked covered in the projection space.

To characterize the shape of a point set, the key is to find its boundary. Consider the sensing sector of S_i which is defined by three vertices S_i, A, B with A being the next vertex of S_i in the counter-clockwise order. Let x_{S_i}, x_A, and x_B denote the corresponding x coordinate of them in the projection space. There are six cases to consider depending on the permutation of the three points (from left to right): (x_{S_i}, x_A, x_B), (x_{S_i}, x_B, x_A), (x_A, x_{S_i}, x_B), (x_A, x_B, x_{S_i}), (x_B, x_{S_i}, x_A), (x_B, x_A, x_{S_i}) (Figure 18).

We consider the first case (Figure 18(a)). It can be further divided into two scenarios depending on if B is the rightmost point of S_i's sensing range. Suppose it is the rightmost point and consider the process that L moves from $x = x_B$ to $x = x_{S_i}$ (Figure 19(a)). There are two parts: the first part from $x = x_{S_i}$ to $x = x_A$ and the second part from $x = x_A$ to $x = x_B$. Recall the two critical positions Q_1 and Q_2 that are the two intersection points of L and S_i's boundary. Here Q_1 is on $\overline{S_iA}$ and Q_2 is on $\overline{S_iB}$ for the first part and $\widehat{BA}$ for the second part. We find the function describing $arg(\vec{Q_1S_i})$ and $arg(\vec{Q_2S_i})$ in terms of L's position $x = x_L$.

Without loss of generality, the coordinate system can be shifted such that $x_{S_i} = 0$. In both the first and the second part, $arg(\vec{Q_1S_i}) = arg(\vec{BS_i})$, which is a constant only depending on the position of S_i and B. In the first part $x_L \in (x_{S_i}, x_A)$, $arg(\vec{Q_2S_i}) = arg(\vec{AS_i})$, which is a constant only depending on the position of S_i and A. In the second part $x_L \in [x_A, x_B)$, $arg(\vec{Q_2S_i}) = \pi - \arccos\frac{x_L}{r}$ (recall r is the sensing radius). Then from the expressions of $arg(\vec{Q_1S_i})$ and $arg(\vec{Q_2S_i})$ and Equation (1), we can define in the projection space the set of points to be marked covered, which is denoted by C_i.

$$\begin{aligned} C_i = \{(x, y) : 0 < x < x_B \text{ and } y_2(x) < y < y_1(x), \text{if } y_2(x) < y_1(x); \\ y_2(x) < y < 2\pi \text{ or } 0 \le y < y_1(x), \text{otherwise}\}, \end{aligned} \tag{3}$$

where

$$\begin{aligned} y_1(x) &= arg(\vec{BS_i}) + \theta \pmod{2\pi}, x \in (x_{S_i}, x_B), \\ y_2(x) &= arg(\vec{AS_i}) - \theta \pmod{2\pi}, x \in (x_{S_i}, x_A), \\ y_2(x) &= \pi - \arccos\frac{x}{r} - \theta \pmod{2\pi}, x \in [x_A, x_b). \end{aligned} \tag{4}$$

Now suppose B is not the rightmost point of S_i's sensing range. In this case, the rightmost point, denoted by B', is on $\widehat{AB}$ (Figure 19(b)). Let $x_{B'}$ be the x coordinate of B' and consider the process when L moves from $x = x_{S_i} = 0$ to $x = x_{B'}$. There are three parts. The first and the second are the same as the preceding; the additional third part is from $x = x_B$ to $x = x_{B'}$. In the third part when Q_1 is on $\widehat{BB'}$ and Q_2 is on $\widehat{AB'}$.

As a result, the set of points to be marked covered in the projection space can be defined similarly as in Equations (3), (4), and the only modification is the additional definition of $y_1(x)$ and $y_2(x)$ in Equation (4), for the additional third part, that is,

$$\begin{aligned} y_1(x) &= \pi + \arccos\frac{x}{r} + \theta \pmod{2\pi}, x \in (x_B, x'_B), \\ y_2(x) &= \pi - \arccos\frac{x}{r} - \theta \pmod{2\pi}, x \in (x_B, x'_B). \end{aligned} \tag{5}$$

We can run similar procedures to find the point sets for the other five cases. Note that although the images of the point sets are not regular shapes like rectangles or triangles, their boundaries are either straight line segments or part of the curve defined by the function arccos(·) that is used in Equations (3), (4), and (5).

6.4. Coverage Verification

As we mentioned, the coverage verification problem becomes the problem asking that in the projection space, whether the subarea A_{proj} defined in Equation (2) is covered by the family of point sets $\{C_i, 1 \le i \le n\}$.

In the projection space, A_{proj} is partitioned into subarea by $\{C_i, 1 \le i \le n\}$. A straightforward method to verify coverage is to go through every subarea and verify the coverage one by one. An alternative considered here is to study the boundary of each C_i.

THEOREM 6.4. *Suppose in the projection space there is at least one C_i whose intersection with $\in A_{proj}$ is nonempty. Then A_{proj} is covered if and only if for each C_i and any point P_B on its boundary and $P_B \in A_{proj}$, P_B is covered by at least one C_j other than C_i.*

PROOF. We will show the "if" part since the "only if" part is obvious.

Suppose the conditions are met but there is one point $P \in A_{proj}$ that is not covered. Note that in our case, A_{proj} is equivalent to $\{(x, y) : x \in (x_{left}, x_{right}), y \in \mathbb{R}(\text{mod } 2\pi)\}$,

which is an open set. A pictorial way to look at A_{proj} is to consider it as the surface of a cylinder, and the boundary, which is composed of the circumference of the bottom and upper disk, does not belong to it. Also, every C_i is essentially an open set in $\{(x, y) : x \in \mathbb{R}, y \in \mathbb{R}(\text{mod } 2\pi)\}$.

As P is an interior point of A_{proj} and it is not covered by any C_i, a connected region R_P (an open set) that contains P and is included in A_{proj} can be found not covered by any C_i. Without loss of generality, suppose R_P is maximal, which means for any point on the boundary of R_P and any neighborhood of the point, there is always a point that is either covered or not in A_{proj}.

Now consider R_P's boundary. There must be a C_i such that the intersection of C_i's boundary and R_P's is nonempty (otherwise R_P is surrounded all by A_{proj}'s boundary which can only happen when $C_i \cap A_{proj} = \emptyset, \forall i$). As a result, for any point on that part of the boundary, it is not covered by any other C_j, $j \neq i$, which is a contradictory. Therefore, A_{proj} is covered. □

7. STRONG BARRIER COVERAGE IN CAMERA SENSOR NETWORKS

In this section, we study the strong barrier coverage problem in camera sensor networks. We will first define what is strong barrier coverage in a camera sensor network. Then a coverage verification algorithm is proposed to determine if the monitored field is under strong barrier coverage. Finally, a heuristic to select cameras to form a camera barrier is given.

7.1. Strong Barrier Coverage of Camera Sensors

Consider a two-dimensional rectangular area A, as in the previous section. A camera sensor network has been deployed to monitor A. The strong barrier coverage of the camera sensor network can be defined as follows.

Definition 7.1. Given a rectangular field A with one side being the entrance and the opposite side being the exit side, A is said to be under strong barrier coverage by the deployed camera sensor network if there is a connected region B inside A such that B is full-view covered and any path from one point on the entrance side to another point on the destination side intersects with B.

With this definition, the barrier coverage verification problem considered here is defined as follows.

Definition 7.2 (*Strong Barrier Coverage Verification*). Given a rectangular field A to be monitored, and a network of camera sensors $S = \{S_1, \ldots, S_n\}$ with predefined sensing radius r and FoV angle φ but arbitrarily chosen locations and orientations, also given the effective angle $\theta \in [0, \frac{\pi}{2})$, the problem asks whether A is under strong barrier coverage by S.

As mentioned in the introduction, simply selecting cameras across the field with connected sensing range does not necessarily form a camera barrier. Besides, compared with the weak barrier coverage considered in the last section, the object's path can be arbitrary and the object's facing direction may also change dynamically during the trip. All of these factors will be taken into consideration in designing an efficient coverage verification algorithm.

7.2. Verification Method Overview

We need to guarantee that each point of the barrier is full-view covered. This is the key challenge here. We approach this problem by first converting the monitored field into a graph (discretization) in which each node represents a small subregion and two nodes are connected if they are adjacent in the original field. By doing this, we can verify the

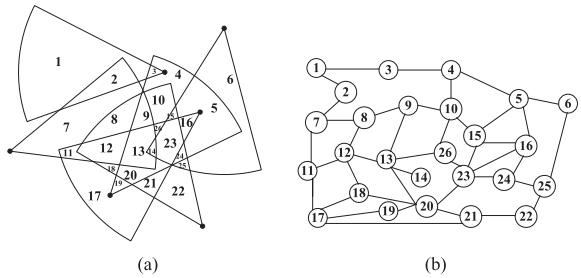

Fig. 20. (a) The monitored area is partitioned into subregions; each subregion is identified by a number; (b) a graph is constructed based on the relationship among the subregions; the number on the node indicates the corresponding subregion in (a).

coverage quality of each subregion and determine a subset of nodes (subregions) that are full-view covered. Then the preceding verification problem is equivalent to asking if there is any path from the left boundary to the right boundary consisting of nodes that are full-view covered. This path represents a set of contiguous subregions across the field, which is essentially the camera barrier we are looking for.

7.3. Discretization

Given a set of deployed sensors, field A can be partitioned into subregions, where each subregion is defined to be a set of points covered by the same set of sensors. Two subregions are adjacent if they share at least one common boundary, which can be a line or arc segment from the boundary of the sensing range of some sensors. We model all the subregions and their relationship to each other by a graph $G = (V, E)$. Each node in V represents a subregion. There is an edge (i, j) between node i and j if and only if they are adjacent subregions. An example of this graph is shown in Figure 20.

Two virtual nodes s and t are then added into this graph. They represent the left and right boundaries of field A, respectively. There is an edge (s, i) between node s and i if subregion i intersects with the left boundary of A. Similarly there is an edge (j, t) if subregion j intersects with the right boundary of A.

The number of subregions in G is $O(n^4)$, where n is the total number of cameras. The reason is as follows. We can consider the field A as a planar graph, where the vertices are the intersection points of sensing sectors and edges are the line or arc segments between any two intersection points. Since any two sensing sectors can have $O(1)$ intersection points on their perimeters, the number of vertices is $O(n^2)$. This further implies the total number of edges is $O(n^4)$. From Euler's formula [Alexandroff 1998], the number of faces, that is, subregions, is thus equal to $2 - O(n^2) + O(n^4)$, which is $O(n^4)$.

7.4. Strong Barrier Coverage Verification

For a given subregion R, we need to verify if every point in it is full-view covered. Note that all points in R are covered by the same set of camera sensors. In this section, we focus on this particular set of sensors. Since R is always within their FoV, we can ignore their orientation vectors (i.e., $\vec{f}_i$). What really matters here is the position of each camera and the geometrical relationship between it and the object's position.

The idea is similar to what we used in Section 3. The difference is that here we apply the verification procedures on each individual subregion rather than on the boundary segments. Similarly as in Theorem 3.4, we have the following result of full-view coverage verification for a subregion R.

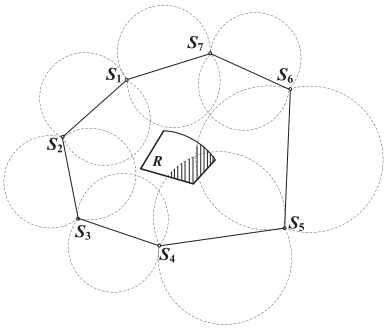

Fig. 21. R is not full-view covered.

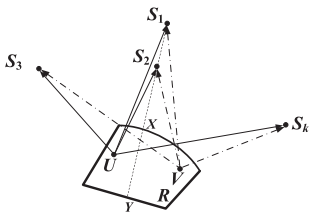

Fig. 22. The circular lists of U and V are different.

THEOREM 7.3. *Suppose R is covered by camera sensors $\{S_{V_1}, \ldots, S_{V_k}\}$, and for every point $V \in R$, the circular list $CL_V = \{S_{V_1}, \ldots, S_{V_k}\}$ is the same (in a circular way/order). Then R is full-view covered if and only if it is within the polygon bounded by $\{\overline{S_{V_i}S_{V_{i+1}}}, 1 \leq i \leq k\}$ and for any $1 \leq i \leq k$, the unsafe region of S_{V_i} and $S_{V_{i+1}}$ does not intersect with R, where V_{k+1} denotes V_1.*

PROOF. This is a direct result by applying Lemma 3.2 and Lemma 3.3 on the subregion R. □

The example in Figure 21 is an illustration of our idea. In this example, there are seven cameras covering subregion R. We draw the boundaries of the unsafe regions for the seven pairs of neighboring sensors (indicated by dotted arcs), as in Lemma 3.3, and check if they intersect with R. Note that in computation this can be done by comparing the distance from the circle's center to each boundary segment of R with the circle's radius. As can be seen in the figure, the unsafe regions of S_4, S_5 and S_5, S_6 intersect with R, and hence the intersection area (shaded area of R) is not full-view covered. All other areas in R are full-view covered.

We still need to consider the issue when the circular list CL_V may not be the same for every point $V \in R$. For example in Figure 22, S_1 is prior to S_2 in V's list, but S_2 is prior to S_1 in U's list, i.e., $CL_V = \{S_1, S_2, S_3, \ldots, S_k\}$, $CL_U = \{S_2, S_1, S_3, \ldots, S_k\}$. This happens if two cameras covering R are on a line which intersects with R (e.g., the line $\overline{S_1S_2}$ intersects with R at X, Y). To solve this problem, we need the following concept.

Definition 7.4 (*Partition*). A partition is a maximal subset of points in a subregion R such that the circular list of every point of the subset is the same.

We need to find all the partitions of R. In fact, R can be partitioned by the lines connecting any two cameras covering R. For example, in the preceding example, R can be divided into two partitions by $\overline{S_1S_2XY}$, where X, Y are the intersection points on R's boundary (note that there will be no new partitions if X, Y are in the middle between S_1 and S_2). If there were another pairs of cameras like this, then R would be further partitioned. For each partition, we can use Theorem 7.3 to verify the coverage.

Once the coverage verification of all subregions have been completed, the graph G will be modified by removing all edges that are adjacent to notes (subregions) not full-view covered. The result graph is called the coverage graph. And the verification result is summarized by the following theorem.

THEOREM 7.5. *If there is an $s-t$ path in the coverage graph, that is, a series of nodes from s to t with each one connected by an edge to the next, in the coverage graph, the monitored field is under strong barrier coverage by the deployed camera sensors.*

PROOF. Obviously, an $s-t$ path in the coverage graph is corresponding to a series of subregions that are all full-view covered and connected together. Also, s (t) represents the left (right) boundary, the node adjacent to s (t) must intersect with the left (right) boundary. Thus, any path from the bottom to the top must intersect with at least one of the preceding subregions. From Definition 7.1, the monitored field is under strong barrier coverage. □

7.5. Discussions

There are several interesting questions that need to be further investigated. We will briefly discuss them as follows.

7.5.1. Minimum Camera Selection. If the monitored field is under strong barrier coverage by the deployed camera sensors, one interesting question is how to find the minimum set of cameras to form the barrier. If we consider this in the coverage graph, there are possibly multiple valid $s-t$ paths in the coverage graph. And we want to select the one (the camera barrier) which requires the minimum number of active cameras.

One way is to count for each $s-t$ path how many cameras needed to full-view cover the selected subregions. However, the number of $s-t$ paths can be an exponential function of the number of nodes, which makes the solution inefficient. In fact, even if we were able to find the path with the minimum cameras used, the path is still not guaranteed to be optimal as some redundancy may exist on the path (see later discussion). This question needs to be further investigated, but here we can use a heuristic based on the shortest-path selection algorithm.

A shortest path between s and t can be found by using Dijkstra's algorithm [Cormen et al. 2001]. There is one implementation issue that is worthy to mention. We observe that two nodes are adjacent if the two subregions share a common boundary. That means the two sets of cameras covering these two subregions differ by only one element, which further implies that one of the two sets includes the other. Thus, if the subregion covered by the larger set is chosen, the other subregion can be covered at no additional cost. During the execution of Dijkstra's algorithm, we take advantage of this property by setting the cost of the edge from the node with a larger camera covering set to the node with a smaller subset to be 0, and all other edges to be 1. This encourages the algorithm to select the node which is covered by cameras that are already selected.

After the shortest path is found, the camera sensors that cover the corresponding sub-regions are activated and all other cameras can be put into sleep.

7.5.2. Redundant Camera Sensors. Another issue is the redundancy in the preceding camera selection algorithm. In general, given a set of selected subregions that are full-view covered by a given set of deployed camera sensors, a camera is considered redundant if the subregions are full-view covered without that camera being used. A subset of cameras are redundant if the subregions are full-view covered after those cameras being removed (turned off). As an illustration, Figure 23 shows the cause of redundancy on an individual subregion. Here, cameras S_1, S_2, S_3 all cover the subregion R, as the unsafe region of the two neighbors of S_3 does not intersect with R, S_3 can be turned off if S_1 and S_2 are both on. Due to this, selecting all the cameras covering the subregion without eliminating possible redundant cameras in the above algorithm might be a waste.

However, the difficulty of removing redundancy is that a camera which is redundant for one subregion may be necessary for another subregion. To resolve the issue,

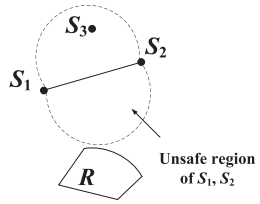

Fig. 23. The cause of redundancy.

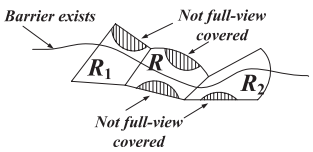

Fig. 24. A barrier across partially covered sub-regions.

redundant cameras for each subregion are first identified. If a subregion has multiple partitions, then each partition is treated separately. A redundant cameras found in one specific subregion (partition) can only be removed if for any other subregions, it is either not used (i.e., it does not cover that subregion) or being a redundant camera in that subregion.

7.5.3. Consideration of Non-Full-View Covered Subregions. Another issue in current coverage verification algorithm is due to the lack of consideration of the subregions that are not full-view covered. It is likely that those subregions may also be used as building blocks for a valid camera barrier. An illustration is shown in Figure 24. In this example, none of the three subregions R, R_1, and R_2 are considered full-view covered. However, since the full-view covered portion of the three is connected, it is still possible to construct a valid barrier across them. Fortunately, the preceding coverage verification procedure proposed can be readily adapted to solve this issue.

The key is to precisely identify for each subregion which part is full-view covered. Without loss of generality, we assume there is only one partition in the subregion. Consider the set of cameras covering a subregion R. Recall that for each pair of adjacent cameras, an arc defining the safe (unsafe) region can be identified (Lemma 3.3). Then consider the intersection of the safe region of all pairs of adjacent cameras covering R, which is denoted by I_R. If I_R is empty, then no point of R is full-view covered. Otherwise, the intersection of I_R and R is the set of points that are full-view covered.

Now for each subregion, there are three possibilities: full-view covered, partially full-view covered with the covered subset identified, and not full-view covered at all. If a subregion is not full-view covered at all, then in the coverage graph, all edges adjacent to the corresponding nodes are removed. If for two adjacent subregions, their fullview covered subsets are connected to each other, the edges between those two subregions are kept. Otherwise, the edge between those two are removed. Finally, after the modification, it can be seen that the monitored field is under strong full-view coverage of the deployed camera sensor network if and only if there is at least one $s - t$ path in the coverage graph.

8. SIMULATION AND NUMERICAL RESULTS

In the simulation, we want to validate the theoretical analysis on sensor density estimation for full-view coverage. Meanwhile, we want to have a pictorial view of the relationship between sensor density and the percentage of full-view coverage. Finally, we will compare barrier coverage and full coverage (i.e., every point of the monitored area is full-view covered) in terms of the number of cameras required.

8.1. Simulation Results on Full Coverage

In this section, we are interested in finding out how many camera sensors are needed to achieve full-view coverage in a random deployment. Note that for a triangle

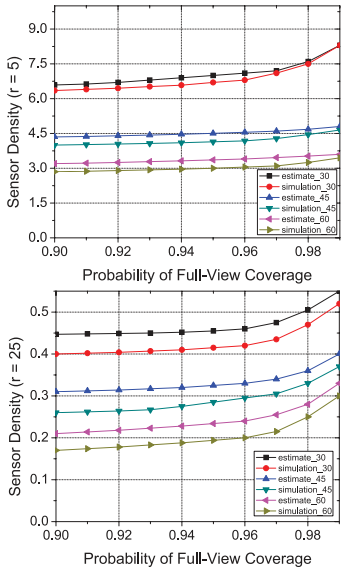

Fig. 25. Density vs. probability ($r = 5, 25$).

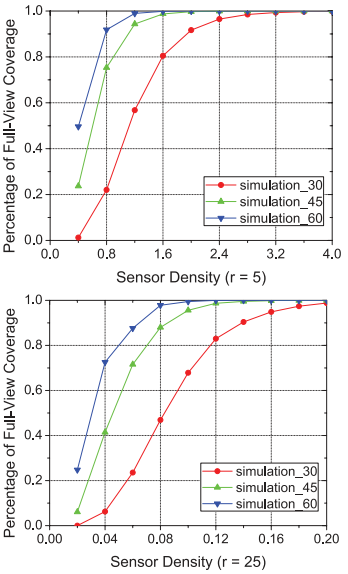

Fig. 26. Percentage vs. density ($r = 5, 25$).

lattice-based deterministic deployment, the numerical result has already been presented in Section 5.

8.1.1. Simulation Configuration. The target field A is a 100m $\times$ 100m square region. We use two settings for sensing radius: $r = 5$ m and $r = 25$ m. In both cases, we deploy the sensors in the field with area of $(100 + 2r)$m $\times$ $(100 + 2r)$m to circumvent the boundary effect. When r is 5 m, it is much smaller compared with the side length, and hence the deployment field is almost the same as A. With $r = 25$ m, it is comparable to the side length, and hence the density results (both in the simulation and theoretical estimation) are for the enlarged deployment field. The FoV angle is fixed to be $\varphi = \pi/3$, and we use three values for the effective angle, that is, $\theta = \pi/6, \pi/4, \pi/3$ (or $30, 45, 60$ in degree) respectively.

In the first step of the simulation, we vary the number of sensors from 10,000 to 90,000 for $r = 5$ m, and from 1,000 to 6,000 for $r = 25$ m, to observe the full-view coverage probability. Each experiment is run 100 times, and the results are averaged. As comparisons, we also give the theoretical estimation for each configuration. Note r is normalized to 0.05 and 0.25, respectively.

In the second step of the simulation, we vary the number of sensors from 4,000 to 40,000 for $r = 5$ m, and from 200 to 2,000 for $r = 25$ m, to observe the percentage of full-view coverage. The percentage of full-view coverage is defined to be the percentage of points that are full-view covered. Each result shown here is the statistical average of 100 experiments.

8.1.2. Simulation Results. Figure 25 shows the results of the sensor density under different probability requirement for full-view coverage. We use the x-axis to denote the probability and the y-axis to denote the sensor density. The results shown here are for probability requirement above 0.9, which would be of interest in practice. The sensor density is normalized by dividing the total number of sensors by the target field's area. The results shown here are for $r = 5$ and $r = 25$. In both cases, the sensor density needed for full-view coverage increases as the required probability increases, although the density for $r = 25$ is much lower than the density for $r = 5$ (reflected by the range

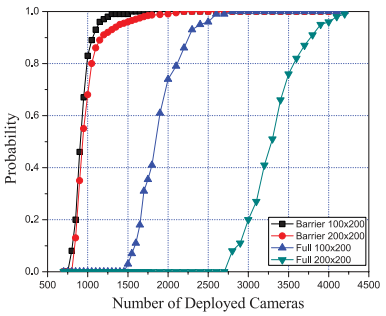

(a) Probability vs. deployed cameras.

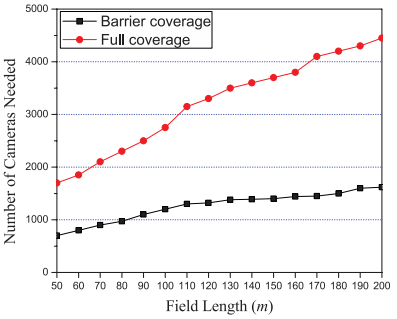

(b) Cameras needed vs. field length.

Fig. 27. Comparison between barrier coverage and full area coverage.

on y-axle). The theoretical results (indicated by 'estimate' in the figures) serve as upper bounds for the real densities (indicated by 'simulation' in the figures) in all cases, which means as long as the sensor density reaches the theoretical bound, the coverage probability is guaranteed. Moreover, the theoretical bounds are very close to the real deployment density. The difference becomes even smaller as the required probability is higher. This further validates the theoretical estimation.

Figure 26 shows the results on the percentage of full-view coverage under different sensor densities. The percentage of full-view covered points increases very quickly as the sensor density increases. By comparing this figure and Figure 25, we can see that although the density needed to achieve full-view coverage for the whole target field may be high, the density needed for a high percentage (but not 100%) of full-view coverage is much lower. For example, when $\theta = \pi/4$ and $r = 25$, 90% of the field is full-view covered when the density is around 0.1 (1,000 sensors). However, if we want to achieve full-view coverage for the whole area with probability 0.9, the density should be above 0.25 (2,500 sensors).

8.2. Simulation Results for Barrier Coverage

In this section, we show the simulation results for the barrier coverage. The main purpose of the simulation is to compare the number of camera sensors needed with full coverage (i.e., every point of the monitored field is full-view covered), and to show the cost effectiveness of the barrier coverage. Only results for strong barrier coverage are shown here, as the results for the weak barrier coverage are similar in trends.

We have two scenarios here. In the first scenario, the monitored field is 200 m in width (along x-axis), 100 m and 200 m in length (y-axis) separately. The camera's parameters are $r = 30$ m, $\theta = \pi/3, \varphi = 2\pi/3$. Cameras are deployed randomly and uniformly in the deployed field. To avoid the boundary effect as we mentioned before, the deployed field is a larger area with both the length and the width $2r$ longer than the monitored filed. Figure 27(a) shows how the coverage probability varies as the number of deployed sensor increases. To estimate the probability, we run each experiment at least 500 times and the probability is obtained by dividing the number of times when the desired coverage is achieved by the total number of tests under each configuration. As Figure 27(a) shows, the probability of the existence of a camera barrier (denoted as "barrier") is almost 1 when the number of cameras deployed is beyond 1,200 if the field length is 100. On the other hand, at least 2,500 cameras are needed for full coverage (denoted as "full"). The difference is even bigger if the field length is 200, where barrier coverage demands no more than 1,700 cameras but full coverage demands more than 4,000 cameras.

In the second scenario, the camera's parameters and the width of the monitored field are fixed as in the preceding. We change the length of the field from 50 m to 200 m and observe how many cameras are needed to achieve the desired coverage (barrier and full) with at least 0.99 probability. Note that in a random deployment given the same number of deployed cameras, as the field length increases, the camera density will drop. As a result, to achieve the same high probability of coverage (in both full and barrier coverage), more cameras should be deployed. As shown in Figure 27(b), the number of cameras required for barrier coverage is much less than that in full coverage. As the field length increases, the number of cameras required for full coverage increases much faster than that for barrier coverage. This result is consistent with our expectation: given the field width unchanged, to achieve full coverage, the area to be full-view covered increases linearly as the field length increases, and so does the number of cameras needed; however since the barrier is across the width of the field, which is unchanged during the test, the number of cameras needed does not increase that fast, and the cost-effectiveness of barrier coverage is obvious.

9. RELATED WORK

Coverage problems under disk sensing model have been studied extensively in the past few years. Under the disk model, coverage detection/verification methods are well studied. In Huang and Tseng [2003] show that an area is k-covered if and only if the perimeter of all sensor's sensing range (disk) is k-covered. A polynomial-time detection algorithm has been proposed based on this perimeter coverage property. In Bejerano [2008], the idea of perimeter coverage has been developed into a distributed protocol in which no location but only distance information is assumed to be known by the sensors. Based on the same assumption, Kasbekar et al. [2009] show that the target field is k-covered if the intersection points of the perimeter of any two sensors' sensing disks are k-covered. They also present a distributed protocol which schedules the sensors to prolong the lifetime of the network with coverage guarantee. More comprehensive surveys on coverage detection (verification) methods can be found [Ahmed et al. 2005; Cardei and Wu 2006]. Another direction on coverage detection is to utilize the property of the Voronoi Diagram. Some interesting works are Cărbunar et al. [2006], Wang et al. [2006], etc.

These studies under disk coverage model inspire our work in this article. Note that like the previously mentioned works, most recent studies in camera sensor networks (e.g., [Hörster and Lienhart 2006; Johnson and Bar-Noy 2011]) still consider cameras as conventional directional sensors. The major difference between theirs and ours is that full-view coverage requires consideration of three factors: the distance between the point and the sensor, the viewing direction of the sensor, and the orientation of the sensor, while in disk model, only the distance needs to be considered. All these issues make the full-view coverage problem much more complicated and challenging.

Barrier coverage was first studied in Gage [1992]. In wireless sensor networks, one related problem is the maximum breach and minimum exposure path problem [Meguerdichian et al. 2001; Li et al. 2003]. In this problem, the coverage quality of a sensor (or exposure) is modeled as a decreasing function of the distance between the sensor and the object. The goal is to find a traversing path in a deployed sensor network such that the maximum exposure is minimized. After the first introduction of the problem, some distributed algorithms have been proposed, in which sensor collaboration is exploited to detect the intruder [Clouqueur et al. 2003; Veltri et al. 2003].

The concepts of weak and strong barrier coverage in wireless sensor networks are introduced in Kumar et al. [2005]. A wireless sensor network provides weak barrier coverage if the intruder is guaranteed to be detected when it takes the shortest path (i.e., an orthogonal line) to cross the field. Strong barrier coverage guarantees the

detection of the intruder no matter what kind of path it takes. They obtain the critical condition of weak barrier coverage in a random deployment. The critical condition for strong barrier coverage is obtained in Liu et al. [2008] by using percolation theory. They also give a distributed algorithm to construct the sensor barrier. An effective way of measuring the quality of barrier coverage is proposed in Chen et al. [2008]. The idea is that if the intruder is guaranteed to be detected when its path is confined in a sliced area with a given width (bounded), then the bound of this width can be used to measure the quality of the barrier. Under this model, the strong barrier coverage and the weak barrier coverage are two extreme cases. They also provide an efficient way to find the weak point of the barrier based on the measurement results. The concept of barrier information coverage is introduced in Yang and Qiao [2009]. The basic idea is to exploit the collaboration between sensors on target detection to reduce the number of sensors in use and hence prolong the network lifetime. Finally, the problem of constructing sensor barrier with mobile sensor is studied in Saipulla et al. [2010]. An optimization algorithm is given to schedule the movement of the mobile sensors for barrier coverage under the constraint that the moving distance of each mobile sensor is limited.

In our work, both the concept of weak and strong barrier coverage have been extended with the consideration of the new features of the full-view coverage model. As we discussed, the differences between camera sensors and traditional scalar sensors in terms of coverage make barrier coverage problem in camera sensor networks much more challenging. And hence it deserves substantial research effort.

10. CONCLUSIONS

Camera sensor networks have drawn much attention recently due to their huge potentials in many applications. One fundamental research issue in camera sensor networks is how to define the coverage. Since traditional disk sensing model does not address the issue of viewing direction, which is intrinsic to camera sensors, in this article we introduced a novel model called full-view coverage. A monitored field is said to be full-view covered if for any point V and an arbitrary facing direction (i.e., a vector $\vec{d}$), there is always a sensor S_i such that V is in S_i's sensing range and the angle between $\vec{d}$ and the direction vector $\overrightarrow{VS_i}$ is smaller than a predefined value θ. With this model, we proposed an efficient method of full-view coverage detection for any given camera sensor network. We also derived a sufficient condition on the sensor density needed for full-view coverage in a random uniform deployment. In addition, we showed a necessary and sufficient condition on the sensor density for full-view coverage in a triangular lattice based deployment.

Based on the full-view coverage model, we also studied the barrier coverage problem of camera sensor networks. The two barrier coverage models in the literature, the weak barrier coverage and the strong barrier coverage, have been extended into two new models by considering the direction issues. Along with the new models, the weak/strong barrier coverage verification problems were introduced, and new detection methods have been proposed.

In this article, we have developed a theoretical framework for the coverage problem in camera sensor networks. The study is far from perfection but just a beginning. We believe that some interesting problems such as the minimum camera selection problem and the redundancy reduction problem in the barrier coverage, and many other related issues have much significance in both research and practice, and hence deserve further investigation.

REFERENCES

AHMED, N., KANHERE, S. S., AND JHA, S. 2005. The holes problem in wireless sensor networks: A survey. *ACM SIGMOBILE Mob. Comput. Commun. Rev. 9,* 2, 4–18.

AKYILDIZ, I. F., MELODIA, T., AND CHOWDHURY, K. R. 2007. A survey on wireless multimedia sensor networks. *Comput. Netw. 51,* 4, 921–960.

ALEXANDROFF, P. S. 1998. *Combinatorial Topology*. Dover, New York.

ALON, N. AND SPENCER, J. H. 2000. *The Probabilistic Method*. John Wiley and Sons.

BEJERANO, Y. 2008. Simple and efficient k-coverage verification without location information. In *Proceedings of the IEEE INFOCOM*. 291–295.

BLANZ, V., GROTHER, P., PHILLIPS, P. J., AND VETTER, T. 2005. Face recognition based on frontal views generated from non-frontal images. In *Proceedings of the IEEE Computer Society Conference on Computer Vision and Pattern Recognition (CVPR'05)*. 454–461.

CAI, Y., LOU, W., LI, M., AND LI, X.-Y. 2009. Energy efficient target-oriented scheduling in directional sensor networks. *IEEE Trans. Comput. 58,* 9, 1259–1274.

CARDEI, M. AND WU, J. 2006. Energy-efficient coverage problems in wireless ad-hoc sensor networks. *Comput. Commun. 29,* 4, 413–420.

CHEN, A., LAI, T. H., AND XUAN, D. 2008. Measuring and guaranteeing quality of barrier-coverage in wireless sensor networks. In *Proceedings of the ACM International Symposium on Mobile Ad Hoc Networking and Computing (MobiHoc'08)*. 2:1–2:31.

CLOUQUEUR, T., PHIPATANASUPHORN, V., RAMANATHAN, P., AND SALUJA, K. K. 2003. Sensor deployment strategy for detection of targets traversing a region. *Mob. Netw. Appl. 8*, 453–461.

CORMEN, T. H., LEISERSON, C. E., RIVEST, R. L., AND STEIN, C. 2001. *Introduction to Algorithms* 2nd Ed. The MIT Press.

CĂRBUNAR, B., GRAMA, A., VITEK, J., AND CĂRBUNAR, O. 2006. Redundancy and coverage detection in sensor networks. *ACM Trans. Sen. Netw. 2,* 1, 94–128.

GAGE, D. 1992. Command control for many-robot systems. In *Proceedings of the 19th Annual AUVS Technical Symposium (AUVS-92)*. 22–24.

HÖRSTER, E. AND LIENHART, R. 2006. On the optimal placement of multiple visual sensors. In *Proceedings of the 4th ACM International Workshop on Video Surveillance and Sensor Networks*.

HUANG, C.-F. AND TSENG, Y.-C. 2003. The coverage problem in a wireless sensor network. In *Proceedings of the 2nd ACM International Conference on Wireless Sensor Networks and Applications*. 115–121.

JOHNSON, M. P. AND BAR-NOY, A. 2011. Pan and scan: Configuring cameras for coverage. In *Proceedings of the IEEE INFOCOM*.

KASBEKAR, G. S., BEJERANO, Y., AND SARKAR, S. 2009. Lifetime and coverage guarantees through distributed coordinate-free sensor activation. In *Proceedings of the ACM Conference in Mobile Computing and Networking (MobiCom'09)*. 169–180.

KERSHNER, R. 1939. The number of circles covering a set. *Am. J. Math. 61,* 3, 665–671.

KUMAR, S., LAI, T. H., AND ARORA, A. 2005. Barrier coverage with wireless sensors. In *Proceedings of the ACM Conference in Mobile Computing and Networking (MobiCom'05)*. 284–298.

LI, X.-Y., WAN, P.-J., AND FRIEDER, O. 2003. Coverage in wireless ad hoc sensor networks. *IEEE Trans. Comput. 52*, 753–763.

LIU, B., DOUSSE, O., WANG, J., AND SAIPULLA, A. 2008. Strong barrier coverage of wireless sensor networks. In *Proceedings of the ACM International Symposium on Mobile Ad Hoc Networking and Computing (MobiHoc'08)*. 411–420.

LIU, C. AND CAO, G. 2011. Spatial-temporal coverage optimization in wireless sensor networks. *IEEE Trans. Mobile Comput. 10,* 4, 465–478.

MEGUERDICHIAN, S., KOUSHANFAR, F., POTKONJAK, M., AND SRIVASTAVA, M. 2001. Coverage problems in wireless ad-hoc sensor networks. In *Proceedings of the IEEE INFOCOM*. 1380–1387.

PHILLIPS, P. J., SCRUGGS, W. T., O'TOOLE, A. J., FLYNN, P. J., BOWYER, K. W., SCHOTT, C. L., AND SHARPE, M. 2007. FRVT 2006 and ICE 2006 large-scale results. Tech. rep. NISTIR 7408, National Institute of Standards and Technology.

RINNER, B. AND WOLF, W. 2008. A bright future for distributed smart cameras. *Proc. IEEE 96,* 10, 1562–1564.

SAIPULLA, A., LIU, B., XING, G., FU, X., AND WANG, J. 2010. Barrier coverage with sensors of limited mobility. In *Proceedings of the ACM International Symposium on Mobile Ad Hoc Networking and Computing (MobiHoc'10)*. 201–210.

SANDERSON, C., SHANG, T., AND LOVELL, B. C. 2007. Towards pose-invariant 2D face classification for surveillance. In *Proceedings of the 3rd International Conference on Analysis and Modeling of Faces and Gestures (AMFG'07)*. 276–289.

SOLOMON, H. 1978. *Geometric Probability*. SIAM, Philadelphia, PA.

SORO, S. AND HEINZELMAN, W. 2009. A survey of visual sensor networks. In *Adv. Multimedia*, 1–22.

VELTRI, G., HUANG, Q., QU, G., AND POTKONJAK, M. 2003. Minimal and maximal exposure path algorithms for wireless embedded sensor networks. In *Proceedings of the ACM SenSys'03*. 40–50.

WANG, G., CAO, G., AND LA PORTA, T. F. 2006. Movement-assisted sensor deployment. *IEEE Trans. Mobile Comput. 5,* 6, 640–652.

WANG, X., XING, G., ZHANG, Y., LU, C., AND GILL, C. 2003. Integrated coverage and connectivity configuration in wireless sensor networks. In *Proceedings of the ACM SenSys'03*. 28–39.

WANG, Y. AND CAO, G. 2011a. Barrier coverage in camera sensor networks. In *Proceedings of the ACM International Symposium on Mobile Ad Hoc Networking and Computing (MobiHoc'11)*. Paris, France, 1781–1789.

WANG, Y. AND CAO, G. 2011b. Minimizing service delay in directional sensor networks. In *Proceedings of the IEEE INFOCOM*. 1790–1798.

WANG, Y. AND CAO, G. 2011c. On full-view coverage in camera sensor networks. In *Proceedings of the IEEE INFOCOM*. 1781–1789.

YANG, G. AND QIAO, D. 2009. Barrier information coverage with wireless sensors. In *Proceedings of the IEEE INFOCOM*. 918–926.

Received May 2012; revised November 2012; accepted January 2013